

## Microscopic picture of aging in SiO<sub>2</sub>

Katharina Vollmayr-Lee,<sup>1,\*</sup> Robin Bjorkquist,<sup>2</sup> and Landon M. Chambers<sup>3</sup>

<sup>1</sup>*Department of Physics and Astronomy, Bucknell University, Lewisburg, Pennsylvania 17837, USA*

<sup>2</sup>*Department of Physics, Cornell University, Ithaca, New York 14853, USA*

<sup>3</sup>*Department of Physics, Texas A&M University, College Station, TX 77843, USA*

(Dated: September 18, 2012)

We investigate the aging dynamics of amorphous SiO<sub>2</sub> via molecular dynamics simulations of a quench from a high temperature  $T_i$  to a lower temperature  $T_f$ . We obtain a microscopic picture of aging dynamics by analyzing single particle trajectories, identifying jump events when a particle escapes the cage formed by its neighbors, and by determining how these jumps depend on the waiting time  $t_w$ , the time elapsed since the temperature quench to  $T_f$ . We find that the only  $t_w$ -dependent microscopic quantity is the number of jumping particles per unit time, which decreases with age. Similar to previous studies for fragile glass formers, we show here for the strong glass former SiO<sub>2</sub> that neither the distribution of jump lengths nor the distribution of times spent in the cage are  $t_w$ -dependent. We conclude that the microscopic aging dynamics is surprisingly similar for fragile and strong glass formers.

PACS numbers: 61.20.Lc, 61.20.Ja, 64.70.ph, 61.43.Fs

If a system is quenched from a high temperature  $T_i$  to a lower temperature  $T_f$  below the glass transition, crystallization is avoided and a glass is formed. The resulting out of equilibrium (aging) dynamics has been hotly debated for the last decades and remains unclear [1, 2]. Most previous studies on the aging dynamics investigated quantities which are averages over all particles in the system, such as mean squared displacement, incoherent intermediate scattering function, dynamic susceptibility, and energy [3–9]. On the other hand much less is known about single particle dynamics during aging. For colloids, Cianci et al. investigated the structure [10, 11] and Yunker et al. [12] focused on irreversible rearrangements as function of waiting time  $t_w$ . Warren and Rottler used computer simulations to investigate single particle hopping events for a binary Lennard-Jones mixture without shear as well as for polymers with and without shear [13–15]. To gain a more complete picture of the microscopic processes during aging, we study single particle hopping (jump) events for the very different glass former SiO<sub>2</sub>. Whereas the systems of Warren and Rottler are fragile glass formers, SiO<sub>2</sub> belongs to the class of strong glass formers [1].

We determine the number of jumping particles per unit time, the jump length, and the time spent in a cage for a wide range of waiting times  $t_w$  and for several choices of  $T_i$  and  $T_f$ . To study the aging dynamics of amorphous silica we carried out molecular dynamics (MD) simulations using the BKS potential [16] for the particle interactions. Starting from 20 independent fully equilibrated configurations at high temperatures  $T_i \in \{5000 \text{ K}, 3760 \text{ K}\}$ , the system is quenched instantaneously to lower temperatures  $T_f \in \{2500 \text{ K}, 2750 \text{ K}, 3000 \text{ K}, 3250 \text{ K}\}$ . To keep the temperature at  $T_f$  constant and to disturb the dynamics minimally, the Nosé-Hoover thermostat was applied only for the first 0.33 ns (NVT), and the simulation was con-

tinued in the NVE ensemble for 33 ns during which  $T_f$  stayed constant. For more information on details of the simulation see [8].

We focus on the microscopic dynamics at the lower temperature  $T_f$  by analyzing the single particle trajectories  $\mathbf{r}_n(t)$ . During the production runs at  $T_f$  we stored average positions  $\bar{\mathbf{r}}_n(t_l)$  and fluctuations  $\sigma_n(t_l) = \sqrt{\mathbf{r}_n^2(t_l) - (\bar{\mathbf{r}}_n(t_l))^2}$  for each particle  $n$  at times  $t_l = l \times (0.00327 \text{ ns})$ . Here  $\overline{(\dots)}$  correspond to averages over 3200 MD steps and 2000 MD steps for the NVT and NVE simulation runs respectively. We then use the resulting  $\bar{\mathbf{r}}_n(t_l)$  to identify jump events. For example Fig. 1 shows the y-component of  $\bar{\mathbf{r}}_n(t_l)$  for  $n = 315$ ; rectangular boxes indicate identified jumps. We define a particle  $n$  to undergo a jump if its change in average position

$$\Delta \bar{r}_n = |\bar{\mathbf{r}}_n(t_l) - \bar{\mathbf{r}}_n(t_{l-4})| \quad (1)$$

satisfies

$$\Delta \bar{r}_n > 3\sigma_\alpha \quad (2)$$

where  $\sigma_\alpha$  is the average fluctuation size for particle type  $\alpha \in \{\text{Si}, \text{O}\}$ . Since  $\sigma_\alpha$  is intended to be a measure of average fluctuations during each particles rattling within its cage of neighbors, we first determine the estimate  $\sigma_{\text{est},\alpha}^2$  by averaging  $(\sigma_n(t_l))^2$  over all times  $t_l$  of a given simulation run at  $T_f$  and over all particles of the same type  $\alpha$ . We then determine  $\sigma_\alpha$  by redoing the average over  $(\sigma_n(t_l))^2$ , but by averaging only over times for which  $(\sigma_n(t_l))^2 < 3\sigma_{\text{est},\alpha}^2$  which roughly excludes jumps from the average. Note that the definition of Eq. (2) is similar, but not identical to our analysis in [17, 18]. To verify that our results are independent of the details of the jump definition, we replaced Eq. (2) with  $\Delta \bar{r}_n > \sqrt{2}\sigma_\alpha$  and found indeed qualitatively the same results as they are presented here, for which we used Eq. (2).

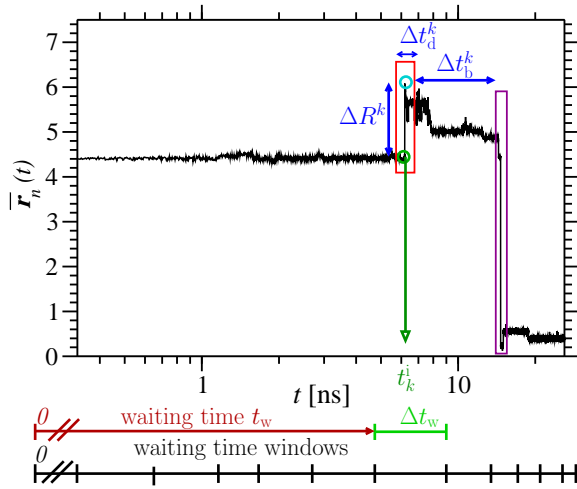


FIG. 1: (Color online) As an example for the time-averaged trajectory  $\bar{\mathbf{r}}_n(t_i)$  we show here the z-component  $\bar{r}_{n,z}$  for the oxygen atom  $n = 315$  for a single simulation run at  $T_f = 2500$  K which had been quenched from  $T_i = 3760$  K. For clarity, only a fraction of the simulation time is shown.

We thus identify for all simulation runs all jump events occurring during the production run at  $T_f$ . For each jump event  $k$  we determine the particle  $n_k$  jumping from average position  $(\bar{\mathbf{r}}_{n_k})^i$  at time  $t_k^i$  to average position  $(\bar{\mathbf{r}}_{n_k})^f$  at time  $t_k^f$  (see in Fig. 1 dark green and cyan circles).

Our focus is on the dynamics of the system as it is aging over time. We investigate it via the jump events and their dependence on the waiting time  $t_w$ , i.e. the time elapsed since the temperature quench to  $T_f$ . We divide the simulation run into waiting time windows, as indicated in Fig. 1 [21]. For each jump event  $k$  with jump time  $t_k^i$  we determine the waiting time window which includes  $t_k^i$  (in Fig. 1 the light green waiting time window) and assign to this waiting time window the waiting time  $t_w$  of the left border of the selected time window (in Fig. 1 red arrow).

We therefore obtain jump statistics for each waiting time window starting at time  $t_w$  and of duration  $\Delta t_w$  (see Fig. 1). In Fig. 2 we show the number of distinct particles jumping per observation time  $\Delta t_w$  as function of waiting time  $t_w$  [22]. We find for all investigated  $T_f$  and both  $T_i$  a clear  $t_w$ -dependence. With increasing waiting time  $\frac{N_p}{\Delta t_w}$  decreases following roughly a power law until equilibrium is reached and  $\frac{N_p}{\Delta t_w}(t_w)$  becomes independent of  $t_w$  and  $T_i$ . The power law exponents are approximately the same for O- and Si-atoms in the range  $[-0.6/\text{ns}, -0.3/\text{ns}]$ . As one might expect, the larger  $T_f$  the more particles jump and the earlier the equilibrium time  $t_{\text{eq}}^i$ , i.e. the time when  $\frac{N_p}{\Delta t_w}$  levels off. For comparison we include in Fig. 2 the equilibrium times  $t_{\text{eq}}^C$  determined via the intermediate incoherent scattering function  $C_q(t_w, t_w + t)$  ( $t_{\text{eq}}^C = t_{23}$  in [8]). We find  $t_{\text{eq}}^i \approx t_{\text{eq}}^C$ , i.e. agreement between the *microscopic* equilibrium time  $t_{\text{eq}}^i$  (single particle jumps) and

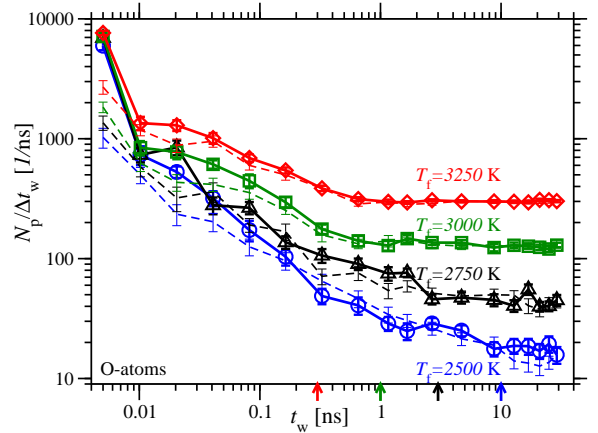


FIG. 2: (Color online) Number of jumping particles  $N_p$  per time  $\Delta t_w$  as function of waiting time  $t_w$  for the case of O-atoms and  $T_i = 5000$  K (bold lines and symbols) and  $T_i = 3760$  K (dashed thin lines). To be able to include on the logarithmic scale the data-point for the first time window at  $t_w = 0$ , we plot  $\frac{N_p}{\Delta t_w}(t_w = 0)$  instead at  $t_w = 0.005$  ns. For comparison the arrows indicate the equilibrium times  $t_{\text{eq}}^C$  ( $t_{23}$  in [8]).

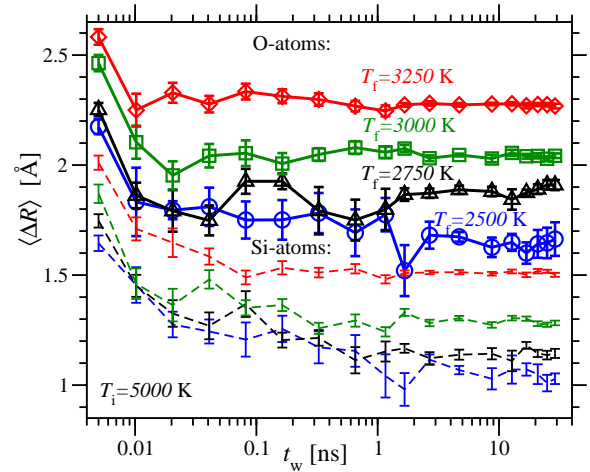


FIG. 3: (Color online) Jump length  $\langle \Delta R \rangle$  (see Eq. (3) and Fig. 1) as function of waiting time  $t_w$  for the case of  $T_i = 5000$  K and O-atoms (bold lines and symbols) and Si-atoms (dashed thin lines). Similar to Fig. 2 we plot  $\langle \Delta R \rangle(t_w = 0)$  at  $t_w = 0.005$  ns.

the *macroscopic* equilibrium  $t_{\text{eq}}^C$  ( $C_q$  includes a particle average).

Next we test whether the  $t_w$ -dependence manifests itself also in a microscopic length scale. As sketched in Fig. 1, we define the jump length of event  $k$  of particle  $n_k$  jumping at time  $t_k^i$  from  $(\bar{\mathbf{r}}_{n_k})^i$  to  $(\bar{\mathbf{r}}_{n_k})^f$  to be

$$\Delta R^k = \left| (\bar{\mathbf{r}}_{n_k})^f - (\bar{\mathbf{r}}_{n_k})^i \right|. \quad (3)$$

Similar to above, we investigate the  $t_w$ -dependence of  $\langle \Delta R \rangle$  by including in the average only events for which  $t_k^i$  belong to the same waiting time window. The resulting Fig. 3 shows that  $\langle \Delta R \rangle$  for oxygen atoms (solid thick

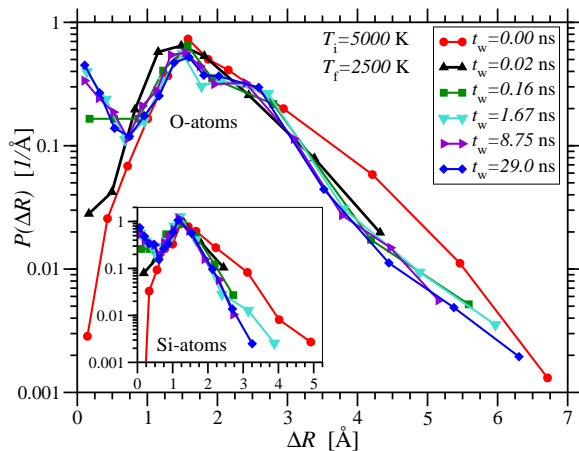


FIG. 4: (Color online) Distribution of the jump length  $P(\Delta R)$  for the case of  $T_i = 5000$  K,  $T_f = 2500$  K and for O-atoms and in the inset for Si-atoms. Different colors indicate waiting time  $t_w$ .

lines with symbols) is independent of  $t_w$  (with the only exception of the first time-window), and for silicon atoms (dashed thin lines)  $\langle \Delta R \rangle$  is only slightly  $t_w$ -dependent. This is in stark contrast to  $\frac{N_p}{\Delta t_w}$  of Fig. 2, which shows strong  $t_w$ -dependence. The  $t_w$ -independence of  $\Delta R$  holds true even for the distribution  $P(\Delta R)$ , both for O- and for Si-atoms, as shown in Fig. 4 for the case of  $T_i = 5000$  K,  $T_f = 2500$  K. We find similar results for all other investigated  $T_i$  and  $T_f$ . Consistent with Fig. 3, we find only  $t_w$ -dependence for  $t_w \lesssim 0.02$  ns (which corresponds in an experiment to the undetectable instant of an infinitely fast quench). For  $t_w > 0.02$  an additional peak occurs at  $\Delta R \approx 0$  which is mostly due to reversible jumps (as defined in [17]). Furthermore we find exponential tails  $P(\Delta R) \sim \exp(-\Delta R/R_{\text{decay}})$  with  $R_{\text{decay}} \approx 0.8$  and  $0.3 \text{ \AA}$  for O- and Si-atoms respectively (similar to the results for a binary Lennard Jones mixture [13]).

With the conclusion from Figs. 3 and 4 that the length scale  $\Delta R$  is  $t_w$ -independent, we investigate next the time scales associated with the single particle jumps. We define the duration of a jump event  $k$  to be

$$\Delta t_d^k = t_k^f - t_k^i \quad (4)$$

(see Fig. 1) and the time between successive jumps of the same particle

$$\Delta t_b^k = t_{k+1}^i - t_k^f \quad (5)$$

that means the time spent in the cage before the same particle jumps again (see Fig. 1). The resulting  $\langle \Delta t_d \rangle$  and  $\langle \Delta t_b \rangle$  are shown in Fig. 5. The time between jumps  $\langle \Delta t_b \rangle$  is several magnitudes larger than  $\langle \Delta t_d \rangle$ . For comparison with  $\langle \Delta t_b \rangle$  we include arrows on the right to indicate  $t_r^{\text{Cq}}(t_w = 23.98 \text{ ns})$  of [8], which is defined to be the time for which  $C_q(t_w, t_w + t_r^{\text{Cq}}) = 0.625$ . Since

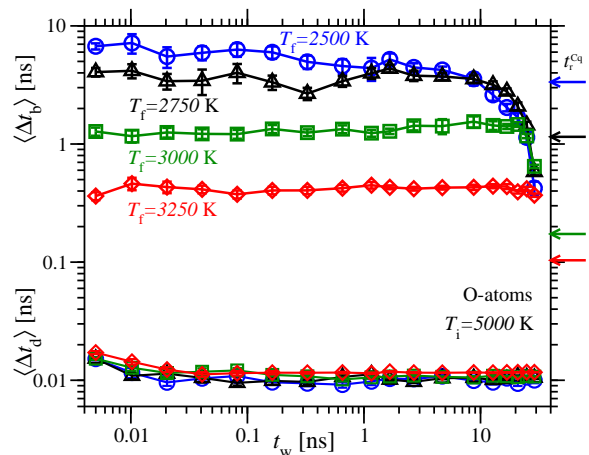


FIG. 5: (Color online) We show here average jump duration  $\langle \Delta t_d \rangle$  (lower four curves) and time between successive jumps of the same particle  $\langle \Delta t_b \rangle$  (top four curves) using the definitions of Eq. (4) and Eq. (5) and Fig. 1. The arrows on the right indicate  $t_r^{\text{Cq}}(t_w = 23.98 \text{ ns})$  of [8]. We include  $\Delta t_d(0 \text{ ns})$  and  $\Delta t_b(0 \text{ ns})$  at  $t_w = 0.005 \text{ ns}$ .

$\langle \Delta t_b \rangle > t_r^{\text{Cq}}$ , we conclude that  $\langle \Delta t_b \rangle$  is characterizing  $\alpha$ -relaxation. As above, we determined the  $t_w$ -dependence by averaging  $\Delta t_d^k$  and  $\Delta t_b^k$  for all jump events  $k$  for which  $t_k^i$  belongs to the same waiting time window. By choosing this definition of  $\langle \Delta t_b \rangle$  we prevent artifacts due to the different time window sizes, because only  $t_k^i$  (instead of  $\Delta t_b^k$ ) is required to be in the time window of consideration. For large  $t_w$ , however, the finite simulation run time  $t_{\text{tot}} = 33.33 \text{ ns}$ , causes  $\langle \Delta t_b \rangle$  to decrease for waiting times  $t_w \gtrsim (t_{\text{tot}} - \Delta t_b)$ . Ignoring this  $t_{\text{tot}}$ -specific decrease, we therefore obtain the surprising result that  $\langle \Delta t_b \rangle$  is independent of  $t_w$ . This independence of  $t_w$  holds not only for the average  $\langle \Delta t_b \rangle$ , but even for the whole distribution  $P(\Delta t_b)$ , as shown in Fig. 6. Also in Fig. 6 we notice that  $P(\Delta t_b) \sim \Delta t_b^{-1}$  at  $T_f = 2500 \text{ K}$ , whereas  $P(\Delta t_b) \sim \exp(-\Delta t_b/t_{\text{decay}})$  at  $T_f = 3250 \text{ K}$ . In Fig. 7 we show how  $P(\Delta t_b)$  plotted versus  $\Delta t_b$  changes with the final temperature, for a fixed  $t_w = 8.75 \text{ ns}$ . We observe that at intermediate temperatures, i.e.  $T_f = 2750 \text{ K}$  and  $T_f = 3000 \text{ K}$ , there is a crossover from power law to exponential decay. For comparison we include in Fig. 7 the same arrows as in Fig. 2, which indicate the equilibrium times  $t_{\text{eq}}^{\text{C}}$ . The crossover time occurs approximately at the same time when  $\frac{N_p}{\Delta t_w}(t_w)$  and  $C_q(t_w, t_w + t)$  reach equilibrium. A similar crossover has been observed for kinetically constrained models (see Fig. 10 of [19]) and for a binary Lennard-Jones mixture (see Fig. 2 of [20]).

In summary, we obtain the following microscopic picture of aging: both the distribution of jump length and the distribution of times spent in the cage  $P(\Delta t_b)$  are independent of waiting time  $t_w$  (similar to the results of Warren and Rottler [13–15]). Instead the only  $t_w$ -dependent microscopic quantity is the number of jump-

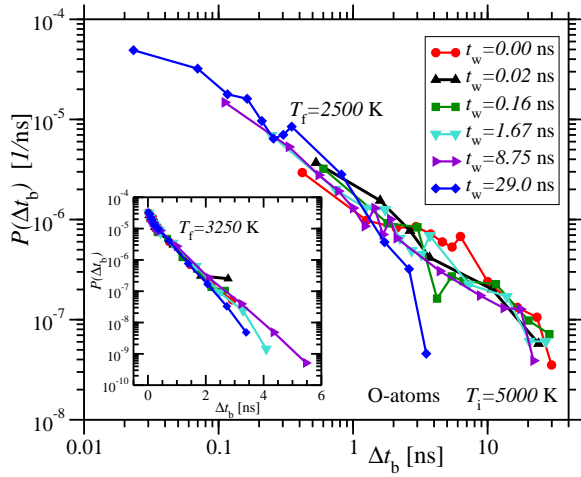


FIG. 6: (Color online) Distribution of times between jumps  $P(\Delta t_b)$  for O-atoms,  $T_i = 5000$  K and for  $T_f = 2500$  K and in the inset for  $T_f = 3250$  K. Different symbols (and colors) correspond to different waiting times  $t_w$ .

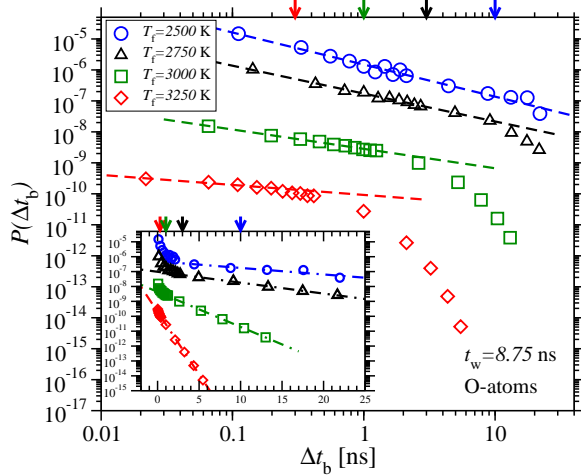


FIG. 7: (Color online)  $P(\Delta t_b)$  for fixed  $t_w = 8.75$  ns,  $T_i = 5000$  K and for O-atoms as log-log plot in the main figure and as log-lin plot in the inset. Different symbols (and colors) correspond to different final temperature  $T_f$ . Dashed lines are power law fits with exponents  $-1.0, -0.9, -0.6, -0.3$  and dot-dashed lines are exponential fits  $P(\Delta t_b) \sim \exp(-\Delta t_b/t_{\text{decay}})$  with  $t_{\text{decay}} = 10, 6, 2, 0.5$  ns for  $T_f = 2500, 2750, 3000, 3250$  K respectively. As in Fig. 2, we include for comparison arrows which indicate the equilibrium times  $t_{\text{eq}}^C$  [8]. For clarity,  $P(\Delta t_b)$  has been shifted by a factor of  $10^{-1}/10^{-3}/10^{-5}$  for  $T_f = 2750/3000/3250$  K respectively.

ing particles per time, which decreases with increasing  $t_w$  (similar to the results of Yunker et al. [12]). This is consistent with the first hop time results reported in [13–15]. In agreement with kinetically constrained models  $P(\Delta t_b)$  shows a crossover from power law to exponential decay [19]. Our results for the strong glass former  $\text{SiO}_2$  are surprisingly similar to the fragile glass former results

[13–15].

RB and LMC were supported by NSF REU grants PHY-0552790 and REU-0997424. We thank A. Zippelius and H.E. Castillo for comments on an earlier version of this manuscript. KVL thanks A. Zippelius and the Institute of Theoretical Physics, University of Göttingen, for hospitality and financial support via the SFB 602.

\* Electronic address: kvollmay@bucknell.edu

- [1] K. Binder and W. Kob, *Glassy Materials and Disordered Solids – An Introduction to Their Statistical Mechanics* (World Scientific, Singapore, 2005).
- [2] L. Berthier and G. Biroli, *Rev. Mod. Phys.* **83**, 587 (2011).
- [3] R. Colin, A. M. Alsayed, J.-C. Castaing, R. Goyal, L. Hough, and B. Abou, *Soft Matter* **7**, 4504 (2011).
- [4] A. Heuer, *J. Phys.: Condens. Matter* **20**, 373101 (2008).
- [5] D. ElMasri, L. Berthier, and L. Cipelletti, *Phys. Rev. E* **82**, 031503 (2010).
- [6] A. Parsaeian and H. E. Castillo, *Phys. Rev. Lett.* **102**, 055704 (2009).
- [7] C. Rehwald, N. Gnan, A. Heuer, T. Schröder, J. C. Dyre, and G. Diezemann, *Phys. Rev. E* **82**, 021503 (2010).
- [8] K. Vollmayr-Lee, J. A. Roman, and J. Horbach, *Phys. Rev. E* **81**, 061203 (2010).
- [9] M. Warren and J. Rottler, *Phys. Rev. E* **78**, 041502 (2008).
- [10] G. C. Cianci, R. E. Courtland, and E. R. Weeks, *Solid State Commun.* **139**, 599 (2006).
- [11] G. C. Cianci, R. E. Courtland, and E. R. Weeks, *AIP Conf. Proc.* **832**, 21 (2006).
- [12] P. Yunker, Z. Zhang, K. B. Aptowicz, and A. G. Yodh, *Phys. Rev. Lett.* **103**, 115701 (2009).
- [13] M. Warren and J. Rottler, *Europhys. Lett.* **88**, 58005 (2009).
- [14] M. Warren and J. Rottler, *Phys. Rev. Lett.* **104**, 205501 (2010).
- [15] M. Warren and J. Rottler, *J. Chem. Phys.* **133**, 164513 (2010).
- [16] B. W. H. van Beest, G. J. Kramer, and R. A. van Santen, *Phys. Rev. Lett.* **64**, 1955 (1990).
- [17] K. Vollmayr-Lee, *J. Chem. Phys.* **121**, 4781 (2004).
- [18] K. Vollmayr-Lee and E. A. Baker, *Europhys. Lett.* **76**, 1130 (2006).
- [19] Y. Jung, J. P. Garrahan, and D. Chandler, *J. Chem. Phys.* **123**, 084509 (2005).
- [20] B. Doliwa and A. Heuer, *Phys. Rev. Lett.* **91**, 235501 (2003).
- [21] In simulation time units ( $1.0217 \times 10^{-5}$  ns) we used the borders  $0, (1000 \times 2^{m_1}$  for  $m_1 = 0, 1, \dots, 6), (64000 + 49500 \times 2^{m_2}$  for  $m_2 = 0, \dots, 3), (64000 + m_3 \times 396000$  for  $m_3 = 2, \dots, 8)$ .
- [22] To avoid that all particles jump, we choose a small enough window. For the case of  $\Delta t_w > 0.506$  ns we therefore divide the waiting time window into subwindows of size  $\Delta t = 0.506$  ns and average over  $\frac{N_p}{\Delta t}$ .